

pubs.acs.org/JACS Article

A Paired-Ion Framework Composed of Vanadyl Porphyrin Molecular Qubits Extends Spin Coherence Times

Casandra M. Moisanu, Hannah J. Eckvahl, Charlotte L. Stern, Michael R. Wasielewski, and William R. Dichtel*



Cite This: J. Am. Chem. Soc. 2024, 146, 28088-28094



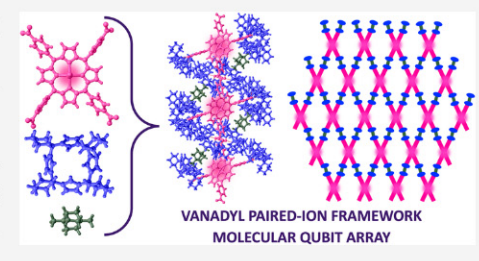
ACCESS

Metrics & More

Article Recommendations

s Supporting Information

ABSTRACT: Molecular electron spin qubits arranged in precise arrays have great potential for use in quantum information science applications. Molecular qubits are synthetically versatile and can be placed in ordered arrangements upon incorporation into a new class of materials known as paired-ion frameworks (PIFs). A PIF composed of vanadyl porphyrin molecular qubits, **VOTCPP-PIF-1**, was synthesized as single crystals. Electron paramagnetic resonance spectroscopy was used to study their spin coherence at temperatures up to 293 K. A suspension of **VOTCPP-PIF-1** at 5 K in dimethylformamide (DMF) had a spin—spin relaxation time ($T_{\rm m}$) of 270 ns. In DMF- d_7 and at 5 K, the coherence time of this material



increased to 370 ns. This increase in $T_{\rm m}$ is attributed to the lower gyromagnetic ratio of $^2{\rm H}$ compared to $^1{\rm H}$, which results in weaker electron–nuclear dipolar coupling that reduces the effect of nuclear spin flips on electron spin coherence. In toluene, crystals of **VOTCPP-PIF-1** had a $T_{\rm m}$ of 31 ns at 293 K, demonstrating that PIFs are a promising platform for creating materials for quantum information science applications.

■ INTRODUCTION

Quantum information science (QIS) involves the control of spin-bearing entities, and its advancement could impact applications such as cryptography and protein modeling. 1-4 As bits are individual units of binary computing, quantum bits, or qubits, are the fundamental units of information for quantum computing.⁵ Many types of qubits have been explored for use in QIS, including superconductors,6quantum dots,⁹ photons, ¹⁰ and nitrogen-vacancy centers. ^{11,12} Molecules are also promising qubit candidates, as they either may contain an unpaired electron or can generate an unpaired electron via a stimulus such as light or electricity. 4,13 Molecular qubits have advantageous characteristics, as they are prepared through chemical synthesis and can be modified rationally to target desired properties.⁴ Furthermore, noncovalent assembly strategies have been used to organize molecular qubits into periodic structures with long-range order, a key feature for applications requiring precise spacing of qubits within an array.4,5,14-17

Supramolecular assemblies, including metal—organic frameworks (MOFs)¹⁸ and two-dimensional polymers (2DPs),^{19,20} have been used to demonstrate the viability of molecular qubits in materials with unique properties. The property used to determine the performance of these materials for QIS applications is the phase memory time, $T_{\rm m}$.²¹ $T_{\rm m}$ is the lower limit of T_2 , the figure of merit in QIS which describes how long qubits maintain a superposition state, also called the coherence time.²¹ For materials to be used for quantum computation, qubits must have a long enough coherence time to carry out

quantum gate operations. 5,21,22 Current strategies to achieve long $T_{\rm m}$ values in framework materials are to use a mixture of metalloporphyrins, in which one porphyrin contains a paramagnetic metal ion while the other contains a diamagnetic metal ion to statistically dilute the paramagnetic metal centers within the framework. 15,17 This approach decreases the density of spins in the material and increases the average distance between spin centers, both of which have been shown to increase coherence time. 15,16,21,23 Although this strategy provided impressive coherence times of up to 122 ns at room temperature, the precise order of molecular qubits, another requirement for quantum computing, is lost. 5

Recently, we reported a paired-ion framework (PIF)^{24,25} with the longest coherence time achieved in a crystalline qubit material that did not rely on qubit dilution.²⁶ PIFs are crystalline supramolecular materials that are held together by interactions between an ion pair receptor, calix[4]pyrrole, ^{27–29} and pairs of molecular ions.^{24,25} Calix[4]pyrroles are macrocycles that can simultaneously bind both anions and cations, ^{27–30} including carboxylates, ³¹ phenolates, ³² sulfates, ³¹ phosphates, ²⁷ quaternary ammoniums, ³³ imidazolium cations, ³⁰ among others. Calix[4]pyrroles can be used to orient

Received: May 29, 2024
Revised: September 20, 2024
Accepted: September 23, 2024
Published: October 3, 2024





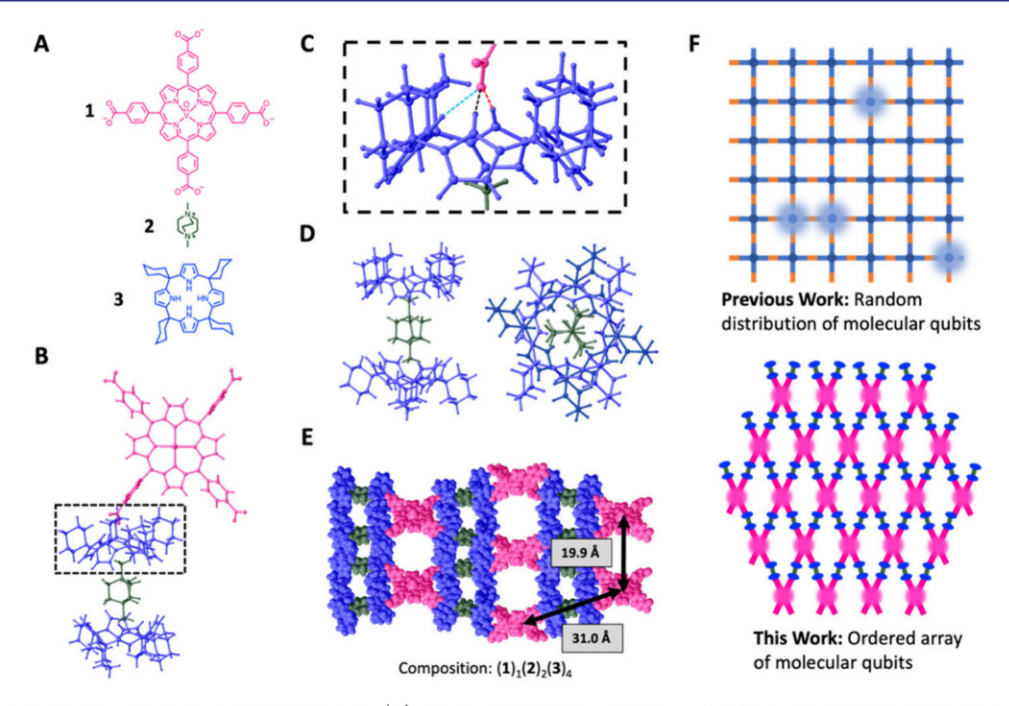


Figure 1. (A) Monomers used to make VOTCPP-PIF-1. (B) Single crystal X-ray structure of a fragment of VOTCPP-PIF-1. (C) Depiction of three hydrogen-bonding interactions at distances of 1.917 Å, 2.050 Å, and 2.003 Å (shown in blue, black, and red dashed lines, respectively) between the carboxylate of 1 and the pyrrole protons of 3. (D) Side (left) and top (right) views of how 2 fits in between two molecules of 3. (E) Single crystal X-ray structure of one sheet of VOTCPP-PIF-1. Distances between vanadyl centers within one sheet are shown. The 19.9 Å distance represents the shortest VO–VO distance in the assembly. Molecules of DMF have been removed for clarity. (F) Cartoon representations of previous supramolecular materials containing molecular qubits randomly distributed throughout the structure and PIFs containing an ordered array of molecular qubits.

pairs of multifunctional monomers into extended, ordered networks called PIFs. 24-26 Given the vast possibilities of ion and calix[4]pyrrole combinations, there are many different structures that could be achieved using this strategy. So far, PIFs have been reported in two classes of structures: ladder polymers, in which the monomers from linear strands held together by host—guest interactions, or two-dimensional sheets that form layered topologies. 24-26 PIFs offer a promising platform for qubit materials because they are composed of light elements with low nuclear spin, and their modularity and durability allows them to be platforms for the exploration of different molecular qubit candidates.

To this end, we sought to use the PIF platform to probe the coherence time of a vanadyl porphyrin-based material. The coherence time of various vanadyl-containing materials has been extensively studied. 15,34,35 Atzori et al. reported a crystalline vanadyl complex with a $T_{
m m}$ of approximately 1 $\mu {
m s}$ at 300 K.³⁴ Vanadyl-containing materials are promising molecular qubit candidates, as their spin-phonon coupling interaction is inefficient, which leads to slower spin-lattice relaxation times. ¹⁵ This spin-lattice relaxation time, T_1 , serves as an upper limit for $T_{\rm m}$; therefore, vanadyl-based molecules make for promising qubit candidates to incorporate into PIFs.4 Here, we report a VO2+ porphyrin-based molecular qubit framework, VOTCPP-PIF-1, composed of VO(II)-tetrakis(4carboxyphenyl)porphyrin (VOTCPP, 1.4H⁺), dimethyl-1,4diazabicyclo[2.2.2.]octane (DM-DABCO, 2.2I-), and tetrakis-(spirocyclohexane)calix[4]pyrrole (3, TSC4P). Electron paramagnetic resonance (EPR) spectroscopy experiments show that this framework exhibits a coherence time of 270 ns at 10 K, a 30% increase from the isostructural Cu based PIF previously reported.²⁶ Additionally, in DMF-d₇, this framework

has a $T_{\rm m}$ of 370 ns, highlighting the effect of removing solvent nuclear spins from qubit materials. Finally, in toluene, **VOTCPP-PIF-1** achieves a $T_{\rm m}$ of 31 ns at 293 K, representing the longest coherence time of a fully saturated array of molecular qubits reported at room temperature.

RESULTS AND DISCUSSION

VOTCPP (1·4H+), DM-DABCO (2·2I-), and TSC4P (3) assemble to form single crystals of VOTCPP-PIF-1 (Figure 1A). The carboxylate substituents on 1 and quaternary ammoniums on 2 make them ideal monomers for forming extended structures when combined with the calix[4]pyrrole host, 3, which simultaneously binds and orients both ions. $^{24-26,30,33}$ $1\cdot 4H^+$, $2\cdot 2I^-$, and 3 were mixed in dimethylformamide (DMF) such that the molar ratio of 1:2:3 was 1:2:133. Tetrabutylammonium methoxide (4 equiv. with respect to 1.4H⁺) was added and after 24 h, red, cubic shaped single crystals of VOTCPP-PIF-1 with side lengths of approximately 50 μ m were observed (Figure S1). Single crystal X-ray diffraction (SCXRD) probed the structure of VOTCPP-PIF-1 (Figure 1B). The solvent masking procedure in Olex2 was used to remove electron density from disordered DMF molecules in the structure.³⁶ In this structure, the carboxylate groups of 1 interact with the three pyrrole protons of 3 at distances of 1.917 Å, 2.050 Å, and 2.003 Å (Figure 1C). Opposite to the carboxylate interactions, an ammonium group of 2 fills in the electron-rich back pocket of 3 (Figure 1C). In VOTCPP-PIF-1, one molecule of 2 sits between two molecules of 3 (Figure 1D, left). These two molecules of 3 are offset by a 45° rotation from one another, resulting in a staggered stacking pattern (Figure 1D, right). The binding arrangement in VOTCPP-PIF-1 is such that each molecule of

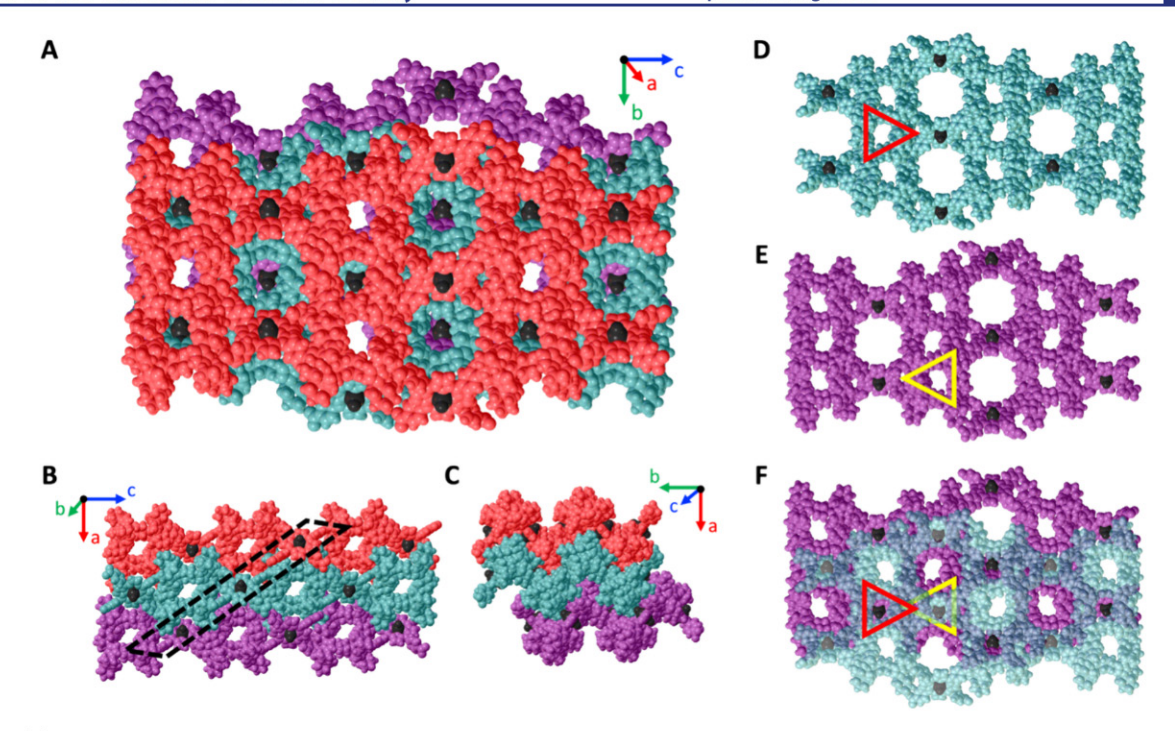


Figure 2. (A) Single crystal X-ray structure of three sheets of VOTCPP-PIF-1 with the same composition as shown in Figure 1E. The top sheet is in red, the middle sheet is teal, and the bottom sheet is purple. Vanadyl centers on all sheets are black. (B) and (C) are alternate views of the same three sheets of (A) shown from different crystallographic orientations. Dashed parallelogram in (B) shows how vanadyl porphyrins stack in columns between layers. (D) and (E) show the teal and purple layers with red and yellow triangles over one pore in the sheet. (F) shows how the teal and purple layers stack together and where the porphyrins from one layer fit within the pores of the other layer.

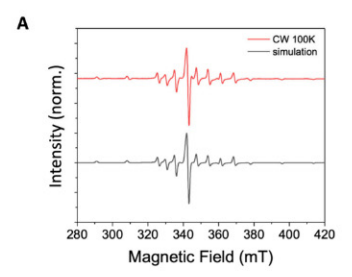
1 is connected to four other molecules of 1 via ion pair interactions between 1, 2, and 3, resulting in the formation of two-dimensional sheets with an empirical formula of $(1)_1(2)_2(3)_4$ (Figure 1E). Within each sheet there are rows of 1 spaced apart such that the VO-VO center distance is 19.9 Å, the closest qubit—qubit distance measured in the framework (Figure 1E). A 10 mL synthesis of VOTCPP-PIF-1 crystals provided a bulk batch of twinned crystals. Capillary powder Xray diffraction (PXRD) of a bulk sample of VOTCPP-PIF-1 closely matches the simulated powder pattern obtained from the single crystal structure obtained from the smaller scale experiment (Figures S2 and S3). The crystals of VOTCPP-PIF-1 contain molecular spin qubits, the paramagnetic vanadyl moiety, distributed throughout the crystal structure (Figure 1F). This approach sets PIFs apart from previous examples of other supramolecular structures such as MOFs15 or polymers 19,37 that contain molecular qubits statistically diluted within the overall material, with no control of intergubit spacing.

Sheets of VOTCPP-PIF-1 stack together to create a crystalline material with precisely placed molecular qubits. One sheet of VOTCPP-PIF-1 is composed of distinct rows of 1 tilted 45° out of the plane of the sheet. (Figure 1E). In one row, all of the molecules of 1 are tilted out of plane in the same direction. In the adjacent rows, the molecules of 1 are tilted the opposite direction, still 45° out of the plane of the sheet. (Figure 1E). Figure 2 shows how sheets of VOTCPP-PIF-1 stack in an ABCD fashion to form the overall crystal structure. Figure 2A-2C shows three layers of VOTCPP-PIF-1 (red, teal, purple) from different crystallographic orientations. The top layer is the same as the sheet shown in Figure 1E. Each layer in this structure is composed of the same unit shown in Figure 1E. Molecules of 2 and 3 form pores in each sheet (highlighted

by a red and yellow triangle in Figure 2D and Figure 2E). Vanadyl centers sit above and below these pores (Figure 2F). The gaps in Figure 2A represent where the vanadyl centers would sit in a sheet below the purple layer and above the red layer. Porphyrins tilted in the same direction form diagonal columns running down the crystal structure (Figure 2B). Molecules of 2 and 3 also form pores 2.4 Å across and 5.9 Å tall running along the sheets of VOTCPP-PIF-1 (Figure 2B). The vanadyl centers of each porphyrin are randomly disordered throughout the crystal structure such that they have a 50% occupancy in either direction of the plane of the porphyrin (Figure 2C) but each porphyrin molecule has a paramagnetic vanadyl center within it.

The viability of VOTCPP-PIF-1 as an ordered array of qubits was assessed using electron paramagnetic resonance (EPR) spectroscopy. This technique probes the spin properties and dynamics of the molecular qubit ensembles. All measurements were done on samples containing many single or twinned crystals of VOTCPP-PIF-1 in DMF at temperatures ranging from 5 to 293 K. Measurements were conducted on samples in DMF because crystals of VOTCPP-PIF-1 would collapse upon solvent removal. Continuous-wave (CW) EPR spectroscopy was conducted on VOTCPP-PIF-1 and showed that incorporation of 1 into a supramolecular structure did not alter its electronic properties. The CW-EPR spectra were simulated using Easyspin assuming a 51V nucleus, axial g tensor and axial hyperfine interaction.³⁸ The values for the g and A tensors were typical for vanadyl porphyrins,³⁹ which indicates that the electronic structure of 1 was not altered upon incorporation into a bulk assembly (Figure 3 and Table S1).

The spin-lattice relaxation time (T_1) of VOTCPP-PIF-1 was investigated using saturation recovery with a picket fence pulse sequence. This parameter represents the thermal



Parameter	Value
g_{\parallel}	1.9592 ± 0.0001
g_{\perp}	1.9834 ± 0.0001
A _∥ (MHz)	481.0 ± 0.4
A _⊥ (MHz)	168.0 ± 0.1
lwpp (mT)	1.14 ± 0.1

Figure 3. (A) CW-EPR spectrum of VOTCPP-PIF-1 collected at 100 K. Experimental data is shown in red, and the best-fit simulation is shown in black. (B) Parameters of the spin Hamiltonian, including the axial g-tensor values, g_{\parallel} and g_{\perp} , the axial hyperfine components coupling to one VO, A_∥ and A_⊥, and the Gaussian line width broadened from peak to peak.

relaxation of qubits, the time it takes for them to relax to their thermal ground state and represents the upper limit for $T_{\rm m}$. The saturation-recovery data used to determine T_1 for

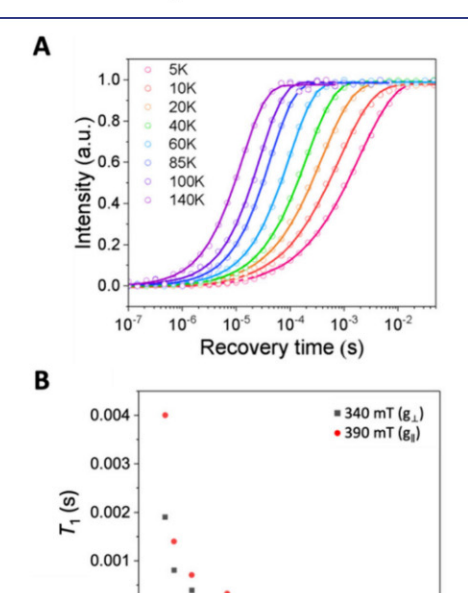


Figure 4. (A) Saturation recovery data from which T_1 is extracted. All data taken at 340 mT, the magnetic field corresponding to g1. Data taken at temperatures ranging from 5 K up to 140 K. At 5 K, the T_1 is 3.1 ms. (B) Plot of T_1 versus temperature at magnetic field corresponding to g_{\perp} (340 mT).

60

Temperature (K)

80 100 120 140 160

VOTCPP-PIF-1 (Figure 4A) was fit to a stretched exponential

$$I(\tau_{recovery}) = 1 - A_0 \exp\left[\left(\frac{-\tau_{recovery}}{T_1}\right)^{\beta}\right]$$

0.000

where I is the echo intensity, A_0 is a constant, and β is the stretch factor that is used to assess the dominant contributions to spin-lattice relaxation. The values for T_1 at different magnetic fields corresponding to g₁ (340 mT) and g₁₁ (390 mT), a magnetic field representing the powder average of the sample and one running along the V=O axis, respectively

(Figure S4 and Table S2). The maximum T_1 at g_{\perp} for VOTCPP-PIF-1 is 2.25 ms and at g_{\parallel} it is 3.20 ms at 5 K (Figure 4B). The values of T_1 decrease as temperature increases due to increased spin-phonon coupling.16 As the temperature increases, the value of β also increases, where β = 1 collapses the fit to a monoexponential decay, indicating spinphonon coupling is the dominant relaxation pathway. A β closer to 0.5 indicates a contribution of cross relaxation from electron spin-spin interactions. 16,19 The highest temperature at which T_1 was recorded for VOTCPP-PIF-1 in DMF was 140 K, and the values for T_1 at this temperature at g_{\perp} and at g_{\parallel} were 12.5 and 17.4 μ s, respectively.

The phase memory lifetime, $T_{\rm m}$, was then characterized using a two-pulse Hahn-echo sequence (Figure 5A). $T_{\rm m}$

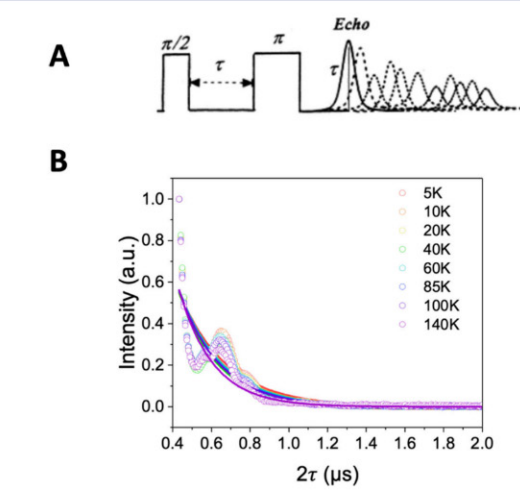


Figure 5. (A) Pulse sequence in which $\tau_{\rm echo}$ is varied to measure $T_{\rm m}$. (B) Hahn-echo data from which $T_{\rm m}$ is extracted at g_{\perp} (340 mT). Experiments were performed at temperatures from 5 to 140 K.

represents the lifetime of the superposition state of a qubit. To confirm that the qubits within VOTCPP-PIF-1 can be placed into a superposition, a nutation pulse sequence was used to drive Rabi oscillations in the system (Figure S5 and Table S3). To determine $T_{\rm m}$, the echo intensity is measured as a function of the interpulse delay time, $\tau_{\rm echo}$, and fitting the data to a monoexponential function

$$I(\tau) = 1 - A_0 \exp\left(\frac{-2\tau}{T_m}\right)$$

(Figure 4B). The $T_{\rm m}$ of VOTCPP-PIF-1 was 270 ns at 5 K and at g_{\perp} . This value represents a 30% increase in $T_{\rm m}$, achieved by replacing a copper(II) cation with an oxovanadium(IV) cation in an isostructural framework.²⁶ Below 30 K, T_m is nearly constant, which is consistent with decoherence due to dipolar or hyperfine interactions. 16,26 The values of $T_{\rm m}$ decrease as temperature increases above 30 K, resulting in $T_{\rm m}$ = 170 ns at g_{\perp} and 140 K. At the highest temperature of this study, $T_{\rm m}$ is not $T_{\rm 1}$ -limited, as the $T_{\rm 1}$ at 140 K is around 40 times larger than $T_{\rm m}$.

In order to probe the effect ${}^{1}H$ atoms on $T_{\rm m}$ in VOTCPP-PIF-1, crystals of the framework were grown in deuterated DMF. Crystals of VOTCPP-PIF-1 contain disordered DMF molecules, whose ¹H atoms can contribute to spin decoherence and therefore shorten T_m.⁴ Indeed, three pulse electron spin-echo envelope modulation (ESEEM) experiments of

VOTCPP-PIF-1 in DMF reveal peaks corresponding to the Larmor frequency of ¹H, indicating that there are unfavorable qubit interactions with protons (Figure S6). Crystals of VOTCPP-PIF-1 were grown in DMF- d_7 (VOTCPP-PIF-1d) to evaluate this effect and further increase $T_{\rm m}$. Previous work by Freedman and co-workers demonstrated that long coherence times of up to 152 μ s can be achieved in molecules with spin-free ligands surrounding vanadyl centers in solvents such as SO₂ to eliminate nearby nuclear spins, which reduces electron-nuclear dipolar coupling, in turn reducing the effect of nuclear spin flips on electron spin coherence.³⁵ Also highlighted was the effect of deuterated solvents on coherence time, as there was a nearly 1.5-fold increase in coherence time of molecules in deuterated solvents compared to nondeuterated solvents.35 Growing the crystals in a deuterated solvent, where ²H has a lower gyromagnetic ratio than ¹H by a factor of 6.5, leads to longer coherence times. 4,40 Indeed, **VOTCPP-PIF-1-d** crystals exhibit a $T_{\rm m}$ of 370 ns at 5 K at g_{\perp} , compared to the T_m of 270 ns of crystals grown in DMF and the same conditions (Figure 6), indicating the role of the

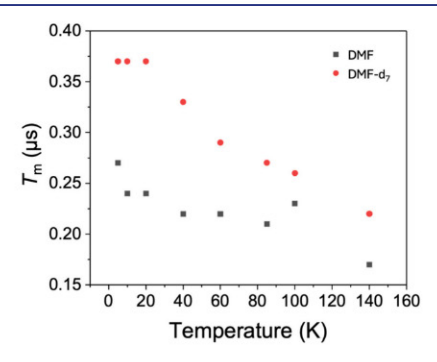


Figure 6. Plot of T_m versus temperature for VOTCPP-PIF-1 in DMF (gray squares) and deuterated DMF (red circles) at g_{\perp} . The $T_{\rm m}$ at 5 K in DMF is 270 ns; the $T_{\rm m}$ at 5 K in DMF- d_7 is 370 ns.

solvent in the relaxation pathway. Even at 140 K, the deuterated crystals of VOTCPP-PIF-1-d have a $T_{\rm m}$ of 220 ns. This finding prompted further probing of the upper limits of temperature at which T_{m} could be elucidated, as the implementation of quantum computing would ideally take place at room temperature, around 293 K.

To push the measurement of $T_{\rm m}$ to room temperature, crystals of VOTCPP-PIF-1 were placed in a mixture of 10% solution of DMF in toluene (v/v). Toluene was chosen because it is a nonpolar solvent that has a low dielectric constant (ε , 2.4) and tan δ (0.040), which means it should absorb less microwave radiation than DMF ($\varepsilon = 37.7$, tan $\delta =$ 0.161) and result in a better signal-to-noise ratio for $T_{\rm m}$ measurements. 41 A mixture of DMF and toluene was needed to maintain the crystal structure of VOTCPP-PIF-1, as powder X-ray diffraction of various samples revealed a change in the crystallinity of VOTCPP-PIF-1 after full solvent exchange in toluene (Figures S2 and S3). CW-EPR of this sample confirms that the vanadyl environment in the crystals does not change in the DMF and toluene mixture (Figures S7 and S8). Crystals of VOTCPP-PIF-1 in the mixture of DMF and toluene exhibit a $T_{\rm m}$ of 31 ns at 293 K (Figure S9). These measurements are the first to report the $T_{\rm m}$ for a homogeneous array of molecular qubits at room temperature.

The $T_{\rm m}$ of VOTCPP-PIF-1 was increased from 270 ns to 1.0 μ s at 5K and g_{\perp} by using a Carr-Purcell-Meiboom-Gill

(CPMG) pulse sequence (Figure 7). This pulse sequence decouples vanadyl centers from nearby electronic or nuclear

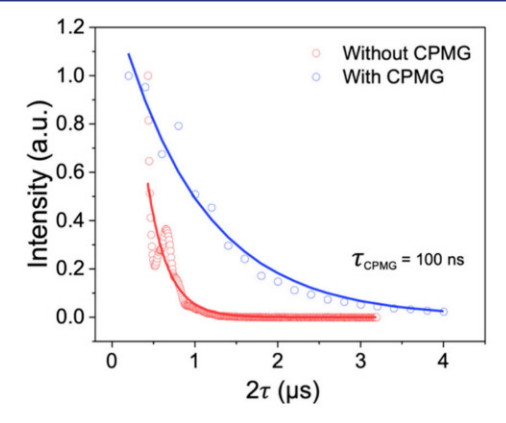


Figure 7. Coherence decay curve obtained using a Carr-Purcell-Meiboom-Gill pulse sequence (blue) and a two-pulse Hahn echo (red) for **VOTCPP-PIF-1**. Via the CPMG method, a T_m of 1.18 μ s is extracted at 5 K and at 340 mT.

spins in the crystal structure. 42 The increase in $T_{\rm m}$ in crystals of VOTCPP-PIF-1 results in a comparable $T_{\rm m}$ to that of a vanadyl MOF, 1.08 μ s for $[VO_{0.02}TiO_{98}(TPP)]$ at the same temperature, reported by Yamabayashi et al. 15 In this MOF, however, only 2% of all porphyrin sites were occupied by a vanadyl group while the rest were occupied by a diamagnetic titanyl group. 15 In VOTCPP-PIF-1, 100% of all porphyrin sites are occupied by a vanadyl group, demonstrating that a homogeneous array of molecular qubits can exhibit long coherence times in a paired-ion framework without the need for diluting with a diamagnetic analogue.

CONCLUSIONS

Paired-ion frameworks (PIFs) offer a promising platform for the exploration of molecular qubit assemblies because they are composed of elements with low nuclear spin and their modularity allows them to be platforms for the exploration of different molecular qubit candidates. Switching from copper to vanadyl-based molecular qubits in an isostructural system allows for the direct comparison of the performance of these molecular qubits in a supramolecular assembly. Crystals of VOTCPP-PIF-1 had a $T_{\rm m}$ of 270 ns, representing a 30% increase from the copper analogue. Measurements of VOTCPP-PIF-1 in deuterated DMF- d_7 showed that the $T_{\rm m}$ of these assemblies can reach 370 ns at 5 K, while studies of these crystals in a mixture of toluene and DMF reveal that they can even exhibit nanosecond-scale coherence at up to 293 K. Further investigations of PIFs as platforms for molecular qubits could include using building blocks with fewer ¹H atoms near the paramagnetic metal ion center in order to further increase the coherence times of these materials or exploring other configurations of the molecular building blocks to create new structures that place molecular qubits in different arrangements.

ASSOCIATED CONTENT

Supporting Information

The Supporting Information is available free of charge at https://pubs.acs.org/doi/10.1021/jacs.4c07288.

Materials and instrumentation, synthetic procedures, single-crystal X-ray diffraction of frameworks, EPR characterization of frameworks, ¹HNMR spectra of monomers, and crystallographic data for VOTCPP-PIF-1 (PDF)

Accession Codes

CCDC 2358096 contains the supplementary crystallographic data for this paper. These data can be obtained free of charge via www.ccdc.cam.ac.uk/data_request/cif, or by emailing data request@ccdc.cam.ac.uk, or by contacting The Cambridge Crystallographic Data Centre, 12 Union Road, Cambridge CB2 1EZ, UK; fax: +44 1223 336033.

AUTHOR INFORMATION

Corresponding Authors

William R. Dichtel - Department of Chemistry, Northwestern University, Evanston, Illinois 60208, United States;

orcid.org/0000-0002-3635-6119; Email: wdichtel@ northestern.edu

Michael R. Wasielewski - Department of Chemistry and Center for Molecular Quantum Transduction, Northwestern University, Evanston, Illinois 60208, United States;

orcid.org/0000-0003-2920-5440; Email: mwasielewski@northwestern.edu

Authors

Casandra M. Moisanu – Department of Chemistry, Northwestern University, Evanston, Illinois 60208, United States; o orcid.org/0000-0001-8760-9991

Hannah J. Eckvahl – Department of Chemistry and Center for Molecular Quantum Transduction, Northwestern University, Evanston, Illinois 60208, United States; o orcid.org/0000-0003-4224-4233

Charlotte L. Stern - Department of Chemistry, Northwestern University, Evanston, Illinois 60208, United States; orcid.org/0000-0002-9491-289X

Complete contact information is available at: https://pubs.acs.org/10.1021/jacs.4c07288

Author Contributions

§C.M.M. and H.J.E. contributed equally to this work.

The authors declare no competing financial interest.

ACKNOWLEDGMENTS

This work was supported by the National Science Foundation under award no. CHE-2154627 (M.R.W.). C.M.M. was supported by an NSF Graduate Research Fellowship under grant DGE-2234667 and the Ryan Fellowship by the International Institute for Nanotechnology (IIN). This research was sponsored by the Army Research Office under Grant Number W911NF-23-1-0306. This work made use of the Integrated Molecular Structure Education and Research Center (IMSERC) at Northwestern University, which has received support from the Soft and Hybrid Nanotechnology Experimental (SHyNE) Resource (NSF ECCS-1542205), the State of Illinois, and the IIN.

REFERENCES

(1) Perdomo-Ortiz, A.; Dickson, N.; Drew-Brook, M.; Rose, G.; Aspuru-Guzik, A. Finding low-energy conformations of lattice protein models by quantum annealing. Sci. Rep. 2012, 2, 571.

- (2) Ladd, T. D.; Jelezko, F.; Laflamme, R.; Nakamura, Y.; Monroe, C.; O'Brien, J. L. Quantum computers. Nature 2010, 464, 45-53.
- (3) Kassal, I.; Whitfield, J. D.; Perdomo-Ortiz, A.; Yung, M.-H.; Aspuru-Guzik, A. Simulating chemistry using quantum computers. Annu. Rev. Phys. Chem. 2011, 62, 185-207.
- (4) Graham, M. J.; Zadrozny, J. M.; Fataftah, M. S.; Freedman, D. E. Forging Solid-State Qubit Design Principles in a Molecular Furnace. Chem. Mater. 2017, 29, 1885-1897.
- (5) DiVincenzo, D. P. The Physical Implementation of Quantum Computation. Fortschritte der Phys. 2000, 48, 771-783.
- (6) Barends, R.; Kelly, J.; Megrant, A.; Veitia, A.; Sank, D.; Jeffrey, E.; White, T. C.; Mutus, J.; Fowler, A. G.; Campbell, B.; et al. Superconducting quantum circuits at the surface code threshold for fault tolerance. Nature 2014, 508, 500-503.
- (7) Murray, C. E. Material matters in superconducting qubits. Mater. Sci. Eng., R 2021, 146, 100646.
- (8) Clarke, J.; Wilhelm, F. K. Superconducting quantum bits. Nature 2008, 453, 1031-1042.
- (9) Kloeffel, C.; Loss, D. Prospects for Spin-Based Quantum Computing in Quantum Dots. Annu. Rev. Condens. Matter Phys. 2013, 4, 51-81.
- (10) Knill, E.; Laflamme, R.; Milburn, G. J. A scheme for efficient quantum computation with linear optics. Nature 2001, 409, 46-52.
- (11) Jelezko, F.; Wrachtrup, J. Single defect centres in diamond: A review. Phys. Stat. Sol. (A) 2006, 203, 3207-3225.
- (12) Childress, L.; Hanson, R. Diamond NV centers for quantum computing and quantum networks. MRS Bull. 2013, 38, 134-138.
- (13) Ferrando-Soria, J.; Magee, S. A.; Chiesa, A.; Carretta, S.; Santini, P.; Vitorica-Yrezabal, I. J.; Tuna, F.; Whitehead, G. F.S.; Sproules, S.; Lancaster, K. M.; Barra, A.-L.; Timco, G. A.; McInnes, E. J.L.; Winpenny, R. E.P.; et al. Switchable Interaction in Molecular Double Qubits. Chem. 2016, 1, 727-752.
- (14) Richardson, C. J. K.; Lordi, V.; Misra, S.; Shabani, J. Materials science for quantum information science and technology. MRS Bull. 2020, 45, 485-497.
- (15) Yamabayashi, T.; Atzori, M.; Tesi, L.; Cosquer, G.; Santanni, F.; Boulon, M.-E.; Morra, E.; Benci, S.; Torre, R.; Chiesa, M. Scaling up electronic spin qubits into a three-dimensional metal-organic framework. J. Am. Chem. Soc. 2018, 140, 12090-12101.
- (16) Yu, C.-J.; Krzyaniak, M. D.; Fataftah, M. S.; Wasielewski, M. R.; Freedman, D. E. A concentrated array of copper porphyrin candidate qubits. Chem. Sci. 2019, 10, 1702-1708.
- (17) Zadrozny, J. M.; Gallagher, A. T.; Harris, T. D.; Freedman, D. E. A Porous Array of Clock Qubits. J. Am. Chem. Soc. 2017, 139,
- (18) Furukawa, H.; Cordova, K. E.; O'Keeffe, M.; Yaghi, O. M. The Chemistry and Applications of Metal-Organic Frameworks. Science 2013, 341, 1230444.
- (19) Oanta, A. K.; Collins, K. A.; Evans, A. M.; Pratik, S. M.; Hall, L. A.; Strauss, M. J.; Marder, S. R.; D'Alessandro, D. M.; Rajh, T.; Freedman, D. E.; et al. Electronic Spin Qubit Candidates Arrayed within Layered Two-Dimensional Polymers. J. Am. Chem. Soc. 2023, 145, 689-696.
- (20) Evans, A. M.; Strauss, M. J.; Corcos, A. R.; Hirani, Z.; Ji, W.; Hamachi, L. S.; Aguilar-Enriquez, X.; Chavez, A. D.; Smith, B. J.; Dichtel, W. R. Two-Dimensional Polymers and Polymerizations. Chem. Rev. 2022, 122, 442-564.
- (21) Yu, C.-J.; von Kugelgen, S.; Krzyaniak, M. D.; Ji, W.; Dichtel, W. R.; Wasielewski, M. R.; Freedman, D. E. Spin and Phonon Design in Modular Arrays of Molecular Qubits. Chem. Mater. 2020, 32, 10200-10206.
- (22) Berliner, L.; Eaton, S.; Eaton, G. Biological magnetic resonance. Distance measurements in biological systems by EPR; Kluwer Academic: New York, 2000; Vol. 19, pp 29-154.
- (23) Wolfe, J. P. Direct Observation of a Nuclear Spin Diffusion Barrier. Phys. Rev. Lett. 1973, 31, 907-910.
- (24) Skala, L. P.; Aguilar-Enriquez, X.; Stern, C. L.; Dichtel, W. R. Dissipative crystallization of ion-pair receptors. Chem. 2023, 9, 709-720.

- (25) Skala, L. P.; Stern, C. L.; Bancroft, L.; Moisanu, C. M.; Pelkowski, C.; Aguilar-Enriquez, X.; Swartz, J. L.; Wasielewski, M. R.; Dichtel, W. R. A modular platform for the precise assembly of molecular frameworks composed of ion pairs. *Chem.* 2023, *9*, 1208.
- (26) Moisanu, C. M.; Jacobberger, R. M.; Skala, L. P.; Stern, C. L.; Wasielewski, M. R.; Dichtel, W. R. Crystalline Arrays of Copper Porphyrin Qubits Based on Ion-Paired Frameworks. *J. Am. Chem. Soc.* **2023**, *145*, 18447–18454.
- (27) Gale, P. A.; Sessler, J. L.; Král, V.; Lynch, V. Calix[4]pyrroles: Old Yet New Anion-Binding Agents. J. Am. Chem. Soc. 1996, 118, 5140–5141.
- (28) Kim, S. K.; Sessler, J. L. Calix[4]pyrrole-Based Ion Pair Receptors. Acc. Chem. Res. 2014, 47, 2525–2536.
- (29) Sessler, J. L.; Gross, D. E.; Cho, W.-S.; Lynch, V. M.; Schmidtchen, F. P.; Bates, G. W.; Light, M. E.; Gale, P. A. Calix[4]pyrrole as a Chloride Anion Receptor: Solvent and Countercation Effects. J. Am. Chem. Soc. 2006, 128, 12281–12288.
- (30) Custelcean, R.; Delmau, L. H.; Moyer, B. A.; Sessler, J. L.; Cho, W.-S.; Gross, D.; Bates, G. W.; Brooks, S. J.; Light, M. E.; Gale, P. A. Calix[4]pyrrole: An Old yet New Ion-Pair Receptor. *Angew. Chem., Int. Ed.* 2005, 44, 2537–2542.
- (31) Park, I.-W.; Yoo, J.; Kim, B.; Adhikari, S.; Kim, S. K.; Yeon, Y.; Haynes, C. J. E.; Sutton, J. L.; Tong, C. C.; Lynch, V. M.; et al. Oligoether-Strapped Calix[4]pyrrole: An Ion-Pair Receptor Displaying Cation-Dependent Chloride Anion Transport. *Chem.—Eur. J.* **2012**, *18*, 2514–2523.
- (32) Sokkalingam, P.; Yoo, J.; Hwang, H.; Lee, P. H.; Jung, Y. M.; Lee, C.-H. Salt (LiF) Regulated Fluorescence Switching. *Eur. J. Org. Chem.* **2011**, 2011, 2911–2915.
- (33) Adriaenssens, L.; Estarellas, C.; Vargas Jentzsch, A.; Martinez Belmonte, M.; Matile, S.; Ballester, P. Quantification of Nitrate-π Interactions and Selective Transport of Nitrate Using Calix[4]pyrroles with Two Aromatic Walls. *J. Am. Chem. Soc.* **2013**, *135*, 8324–8330.
- (34) Atzori, M.; Morra, E.; Tesi, L.; Albino, A.; Chiesa, M.; Sorace, L.; Sessoli, R. Quantum Coherence Times Enhancement in Vanadium(IV)-based Potential Molecular Qubits: the Key Role of the Vanadyl Moiety. *J. Am. Chem. Soc.* **2016**, *138*, 11234–11244.
- (35) Yu, C.-J.; Graham, M. J.; Zadrozny, J. M.; Niklas, J.; Krzyaniak, M. D.; Wasielewski, M. R.; Poluektov, O. G.; Freedman, D. E. Long Coherence Times in Nuclear Spin-Free Vanadyl Qubits. *J. Am. Chem. Soc.* **2016**, *138*, 14678–14685.
- (36) Dolomanov, O. V.; Bourhis, L. J.; Gildea, R. J.; Howard, J. A. K.; Puschmann, H. *OLEX2*: a complete structure solution, refinement and analysis program. *J. Appl. Crystallogr.* **2009**, 42, 339–341.
- (37) Xu, H.; Zhang, Y.; Wang, M. Tunable Quantum Coherence of Polymer-Attached Molecular Spins (PAMS): An Example of Metal-Porphyrin-Centred Four-Arm Star-Like Polymers. *Macromolecules* **2024**, *57*, 2628–2638.
- (38) Stoll, S.; Schweiger, A. EasySpin, a comprehensive software package for spectral simulation and analysis in EPR. *J. Magn. Reson.* **2006**, *178*, 42–55.
- (39) Kivelson, D.; Lee, S. K. ESR Studies and the Electronic Structure of Vanadyl Ion Complexes. *J. Chem. Phys.* **1964**, *41*, 1896–1903
- (40) Haynes, W. M. CRC handbook of chemistry and physics; CRC Press: 2014.
- (41) Gabriel, C.; Gabriel, S. H.; Grant, E. H.; Grant, E. S. J.; Halstead, B.; Michael, P.; Mingos, D. Dielectric parameters relevant to microwave dielectric heating. *Chem. Soc. Rev.* 1998, 27, 213–224.
- (42) Meiboom, S.; Gill, D. Modified Spin-Echo Method for Measuring Nuclear Relaxation Times. *Rev. Sci. Instrum.* **1958**, 29, 688–691.